

Plastic modeling with nonlocal damage of concrete subject to mechanical loading

A. Mohamad-Hussein & J. F. Shao

Laboratory of Mechanics of Lille, Cité Scientifique, 59655 Villeneuve d'Ascq, France

ABSTRACT: Damage due to growth of microcracks is the essential failure mechanism in concrete. Different damage models (phenomenological and micromechanical approaches) have been developed for damage modelling in concrete under mechanical loading. Due to heterogeneity of microstructure, local tensile stresses can be generated during loading leading to growth of microcracks and failure. In this paper, we present an elastoplastic model with non-local damage for the description of mechanical behavior and failure process in concrete due to mechanical loading. The non-local formalism is used in order to describe material behaviour after onset of strain localization. After the calibration of the model from typical laboratory data, comparison between experimental data and numerical simulations are presented. The proposed model is implemented in a FEM code. The failure process of a concrete beam subjected to vertical point force applied on the top surface is analysed. Both local and non-local analyses are performed. The results show that the non-local formalism is capable of regularizing the strain localization and failure process.

1 INTRODUCTION

Concrete materials present elastoplastic damage behaviour. Extensive experimental investigations have been realized on concrete to understand the behaviour of such type of materials. The elastic and plastic properties are affected by induced damage, which leads to a softening behaviour. The behaviour of concrete depends on the confining pressure. Under low confining pressure, failure due to coalescence of microcracks is the main mechanism. Whereas, under high confining pressure, the plastic deformation becomes the main mechanism, and hence, there is a clear transition from ductile to brittle behaviour. Mechanical behavior is also clearly different between tensile and compressive stresses. Coupled plastic deformation and induced damage model should be used for the description of concrete under various loading conditions. The mechanism of failure is not related only to that of plastic deformation. The failure of concrete is generally related to the strain localization phenomenon which leads to a softening behavior. It is then important to describe the post localization behaviour of the material for a sound description of failure process. In quasi-brittle materials like concrete, the material softening is generally viewed as a consequence of the damage due to nucleation and growth of microcracks. This feature should be taken into account in the constitutive model.

From a numerical point of view, some severe difficulties arise and can be noticed in softening modeling. The analysis shows a great dependence of the results on the mesh distribution. The strain or damage localizes into a band within the mesh. The width of this band decreases and tends to zero when the mesh is refined. The boundary value problem becomes ill-posed due to the loss of ellipticity (Hill & Hutchinson 1975). The non-local approach was developed in order to regularize the problem of strain localization and mesh sensitivity (Pijaudier-Cabot & Bazant 1987). In this approach, the constitutive law for damage description at a point of a continuum involves weighted averages of a state variable over a certain neighbourhood of that point. The non-local approach must be applied to the variables that cause strain softening and not to the elastic behaviour. A characteristic length is introduced in order to fix the width of the failure process zone in which strain localizes (Bazant & Pijaudier-Cabot 1989). This will prevent strain localization into a band of zero-width.

The present paper presents the formulation of an elastoplastic with non local damage model. A non associated flow rule is used together with plastic strain hardening law. The material softening is supposed to be related to the damage induced by microcracks. The model takes into consideration the coupling between the elastic - plastic deformation and damage. The model is then extended to a non-

local one. Comparisons between experimental data and the response of the model are presented. A numerical application for a boundary value problem is provided in order to show the performance of the model. However, only mechanical loading is considered in the present paper. Extension to coupled hydromechanical and chemo-mechanical loading will be presented in future papers.

2 FORMULATION OF THE MODEL

In this section, we present the formulation of a local elastoplastic damage model. The constitutive behaviour law is formulated by adopting the assumption of small strains. The total strain tensor, $d\bar{\varepsilon}$, is decomposed into an elastic part, $d\bar{\varepsilon}^e$, and a plastic part, $d\bar{\varepsilon}^p$:

$$d\bar{\varepsilon} = d\bar{\varepsilon}^e + d\bar{\varepsilon}^p \quad (1)$$

2.1 Elastic behaviour

The effective elastic behaviour is characterized by the bulk modulus, $k(d)$, and the shear modulus, $\mu(d)$. Those two moduli are degraded by the induced damage. Based on micromechanical analysis (Mura 1987), they are supposed to depend on the damage variable, d as follows:

$$k(d) = k_0[1 - \alpha_1 H(\varepsilon_v^e) d], \quad \mu(d) = \mu_0[1 - \alpha_2 d] \quad (2)$$

k_0 and μ_0 are the initial bulk and shear moduli respectively, α_1 and α_2 are two parameters that define the progressive deterioration of elastic properties due to damage. ε_v^e is the elastic volumetric strain and $H(\varepsilon_v^e)$ is the Heaviside's function introduced to describe unilateral effect of crack closure on bulk modulus.

The thermodynamic potential is the sum of the energy for elastic strain and the locked energy for plastic hardening:

$$\Psi(\varepsilon^e, \gamma_p, d) = \frac{1}{2} [k(d)(\varepsilon_v^e)^2 + 2\mu(d)\bar{e}^e : \bar{e}^e] + \Psi^p(\gamma_p) \quad (3)$$

ε_v^e is the elastic volumetric strain, \bar{e}^e is the elastic deviatoric strain tensor, γ_p is the generalized plastic shear strain and $\Psi^p(\gamma_p)$ is the locked energy for plastic hardening. We assume, in the present model, that the evolution of damage is not coupled with the plastic hardening process. So, the locked energy for plastic hardening is independent of the damage variable. The constitutive equations are obtained by the standard derivation of the thermodynamic potential with respect to elastic strain:

$$\bar{\sigma} = \frac{\partial \Psi}{\partial \bar{\varepsilon}^e} = k(d) \text{tr}(\varepsilon^e) \bar{\delta} + 2\mu(d) \bar{e}^e \quad (4)$$

2.2 Plastic characterization

The plastic behaviour of concrete depends generally on three invariants of stresses: the average stress, the deviatoric stress and Lode's angle, defined by:

$$I = -\text{tr}(\bar{\sigma}), \quad \bar{\sigma} = \sqrt{3J_2}, \quad \theta = \frac{1}{3} \text{Sin}^{-1} \left(-\frac{3\sqrt{3}J_3}{2J_2^{3/2}} \right)$$

$$\bar{s} = \bar{\sigma} - \frac{\sigma_{kk}}{3} \bar{\delta}, \quad J_2 = \sqrt{\frac{3}{2} s_{ij} s_{ij}}, \quad J_3 = \det(\bar{s}) \quad (5)$$

\bar{s} denotes the tensor of deviatoric stress.

Based on experimental data, the mechanical behaviour of concrete depends strongly on the confining pressure. So, it appears appropriate to use a non linear yield surface for the description of such kind of materials. The quadratic failure surface proposed by Pietruszczak et al. (Pietruszczak et al. 1998) is adapted in the present model:

$$F = c_{10} \left(\frac{\bar{\sigma}}{g(\theta)f_c} \right) + c_{20} \left(\frac{\bar{\sigma}}{g(\theta)f_c} \right)^2 - \left(c_{30} + \frac{I}{f_c} \right) = 0 \quad (6)$$

c_{10} , c_{20} , and c_{30} are model parameters of sound material that define the geometrical form of the failure surface in stress space. The three parameters define material cohesion and friction coefficient. f_c represents the uniaxial compressive strength of the material. θ is Lode's angle defined within the interval $\theta \in \left[-\frac{\pi}{6}, \frac{\pi}{6} \right]$. $g(\theta)$ permits to take into account the influence of the third invariant of stress on the failure surface. This function satisfies the aspect ratio condition $g(\frac{\pi}{6}) = 1$ and $g(-\frac{\pi}{6}) = K$. K is a material parameter defined by the ratio of the slope of the tensile meridian to the compressive one.

We used the function proposed by William and Warnke (William & Warnke 1975) for the definition of Lode's function:

$$g(\theta) = \frac{2(1-K^2)\text{Cos}\left(\theta + \frac{\pi}{6}\right) + (2K-1)\sqrt{4(1-K^2)\text{Cos}^2\left(\theta + \frac{\pi}{6}\right) + 5K^2 - 4K}}{4(1-K^2)\text{Cos}^2\left(\theta + \frac{\pi}{6}\right) + (2K-1)^2} \quad (7)$$

The failure surface is convex for all values of K between 0.5 and 1 (Fig. 1).

Damage by microcracks affects the material behaviour, especially the plastic and failure properties. In order to account for damage effect on plastic deformation, it assumed that the compressive

strength of material, f_c , decreases with the increase of damage. This is in agreement with experimental data observed on various concrete. However, for the sake of simplicity, the following linear relation is used:

$$f_c = f_{c0}(1 - d) \quad (8)$$

f_{c0} denotes the uniaxial compressive strength of undamaged material and d is the damage variable. Replacing f_c in (6) using (8), we can obtain the expression of failure surface for damaged material:

$$F = c_1 \left(\frac{\bar{\sigma}}{g(\theta)f_{c0}} \right) + c_2 \left(\frac{\bar{\sigma}}{g(\theta)f_{c0}} \right)^2 - \left(c_3 + \frac{I}{f_{c0}} \right) = 0 \quad (9)$$

with:

$$c_1 = c_{10}, c_2 = \frac{c_{20}}{(1 - d)}, c_3 = c_{30}(1 - d) \quad (10)$$

We notice that the material cohesion and friction are affected by the induced damage.

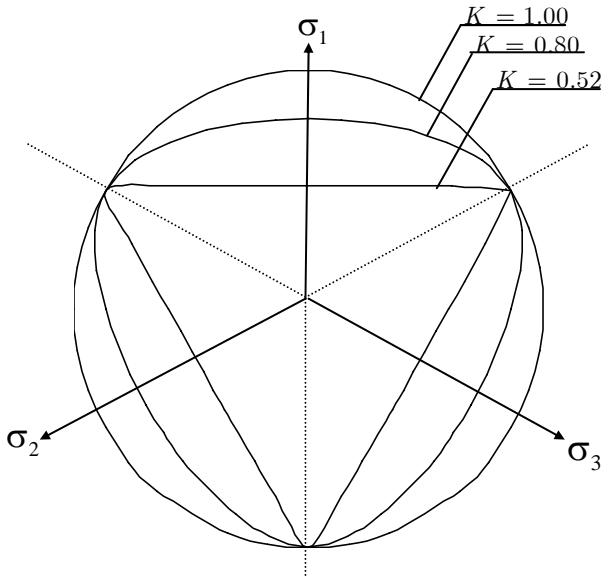


Figure 1. Representation of the plastic loading surface in the principal deviatoric stress space for different values of K .

By supposing that the failure surface represents the asymptotic position of the plastic loading surface, and by introducing a plastic hardening law, the plastic yield function can be written in the following parametric form:

$$f_p = \bar{\sigma} - \alpha_p(\gamma_p)g(\theta)\bar{\sigma}_c = 0 \quad (11)$$

with:

$$\bar{\sigma}_c = \frac{-c_1 + \sqrt{(c_1^2 + 4c_2(c_3 + I/f_{c0}))}}{2c_2} f_{c0} \quad (12)$$

$\alpha_p(\gamma_p)$ represents the plastic hardening law. Its expression is deduced from the locked plastic

potential $\Psi^p(\gamma_p)$. The latter is a function of the plastic hardening variable γ_p . Based on experimental data from compression tests on concrete materials, the locked plastic energy function is expressed as follows:

$$\Psi^p(\gamma_p) = \gamma_p - A_0 \ln \left(\frac{A_0 + \gamma_p}{A_0} \right) \quad (13)$$

The parameter A_0 controls the kinetics of plastic hardening. The standard derivation of the locked plastic potential with respect to γ_p gives us the expression of the plastic hardening law.:

$$\alpha_p(\gamma_p) = \frac{\gamma_p}{A_0 + \gamma_p} \quad (14)$$

Therefore, the hardening law $\alpha_p(\gamma_p)$ is an increasing hyperbolic function of the plastic distortion γ_p .

The generalized plastic shear strain γ_p is defined by:

$$d\gamma_p = \frac{\sqrt{\frac{2}{3} d\bar{e}^p : d\bar{e}^p}}{\chi_p}, \quad d\bar{e}^p = d\bar{\varepsilon}^p - \frac{1}{3} tr(d\bar{\varepsilon}^p) \bar{\delta} \quad (15)$$

$d\bar{e}^p$ is the deviatoric plastic strain tensor. The function χ_p is introduced for the case where the plastic hardening rate depends strongly on the confining pressure. It is defined as:

$$\chi_p = \left(\frac{\langle I \rangle + f_{co}}{f_{co}} \right)^{b_1} \quad (16)$$

$\langle \rangle$ represents Macauley brackets and b_1 is a model's parameter.

According to experimental data for concrete, there is a necessity to use a non associated plastic flow rule in order to describe correctly the plastic compressibility and dilatancy. Inspired by the plastic model proposed by Pietruszczak et al. (Pietruszczak et al. 1988) for concrete, the following plastic potential is used:

$$Q = \bar{\sigma} + \mu_c g(\theta) \bar{I} \ln \left(\frac{\bar{I}}{\bar{I}_0} \right) = 0, \quad \bar{I} = c_3 f_{co} + I \quad (17)$$

\bar{I}_0 is a coefficient that corresponds to the intersection point between the plastic potential surface and the axis $\bar{I} > 0$. μ_c represents the ratio $\frac{\bar{\sigma}}{g(\theta)\bar{I}}$ at the point for which $d\varepsilon_{kk}^p = 0$; i.e. the

transition point from plastic compressibility to dilatancy.

2.3 Damage characterization

The induced damage is supposed to be isotropic for the sake of simplicity. However, the induced damage is generally anisotropic for concrete materials subjected to compressive loading due to the distribution and the orientation of microcracks.

The evolution of damage is determined through a damage criterion. A driving force is supposed to be responsible of the damage evolution. Referring to the previous work performed by Mazars on the damage of concrete (Mazars 1984), an exponential form was chosen for describing the damage criterion:

$$f_d(\xi_d, d) = d_c - d_c \exp[-B_d(\xi_d - \xi_0)] - d \leq 0 \quad (18)$$

d_c represents the critical damage. It corresponds to the residual strength of the damaged material. ξ_0 is the initial threshold of damage. B_d is a parameter that controls the kinetics of the evolution of damage.

The damage evolution of concrete materials, under compression, is affected by both elastic and plastic strains. Therefore, the driving force of damage, ξ_d , is supposed to depend on total strain. It depends on the volumetric dilatance strain and the shear strain:

$$\xi_d = \frac{1}{2} [\alpha_1 k_0 \langle \varepsilon_v \rangle^2 + 2\alpha_2 \mu_0 \bar{\varepsilon} : \bar{\varepsilon}] / \chi_d \quad (19)$$

χ_d describes the effect of the confining pressure on the damage evolution and the transition from brittle to ductile behaviour. We have proposed the following expression for the normalizing function:

$$\chi_d = \left(\frac{\langle I \rangle + f_{co}}{f_{co}} \right)^{b_2} \quad (20)$$

b_2 is a model's parameter. With this normalizing function, the rate of damage becomes smaller when confining pressure is higher. Then there is a transition from brittle behaviour under low confining pressure to ductile behavior under high confining pressure.

3 NUMERICAL SIMULATIONS

The proposed model contains 14 parameters. Those parameters can be fully identified from a series of triaxial compression tests with different confining pressures. In Table 1, we present the values of the

parameters for the concrete data reported by Kotsovos and Newman (Kotsovos & Newman 1980).

Table 1. Model parameters for concrete material reported by Kotsovos and Newman (Kotsovos & Newman 1980)

Parameter	Value		
	MPa	No unit	Pa ⁻¹
E_0	300000		
ν_0		0.15	
f_{c0}	46.9		
c_{10}		1.5	
c_{20}		0.102	
c_{30}		0.714	
b_1		1.0	
A_0		0.0003	
μ_c		0.466	
K		0.68	
d_c		0.8	
ξ_0	0.0605		
B_d			6.10 ⁻⁸
b_2		1.0	

Figure 2 presents the comparison between the failure surfaces for triaxial compression and extension tests with the experimental data reported by (Smith 1985, Mills & Zimmerman 1970, Imran 1994, Scholz et al. 1995, Linse & Aschl 1976, Sfer et al. 2002). The following comparison shows the capacity of the model to describe the behaviour at the ultimate stress state for concrete materials.

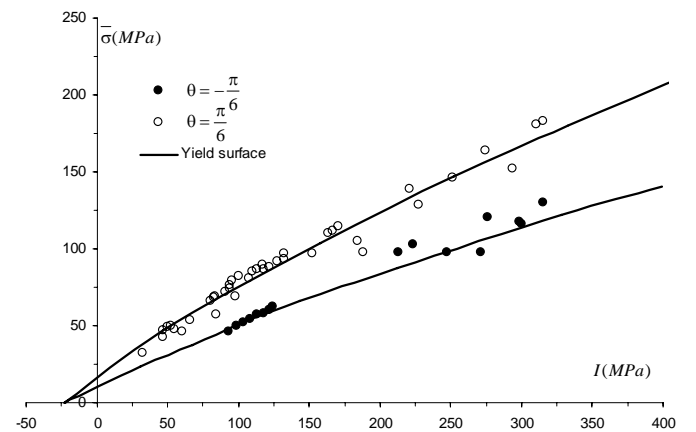


Figure 2. Compressive and tensile failure surfaces in $(I, \bar{\sigma})$ plane. Data from (Smith 1985, Mills & Zimmerman 1970, Scholz et al. 1995, Linse & Aschl 1976, Sfer et al. 2002).

Another comparison is done in the deviatoric plane. This comparison was performed in order to show the capability of the proposed failure criterion to describe correctly the failure of concrete in different loading orientations along Lode's angle. There is a good agreement between the numerical response and the experimental data (Fig. 3).

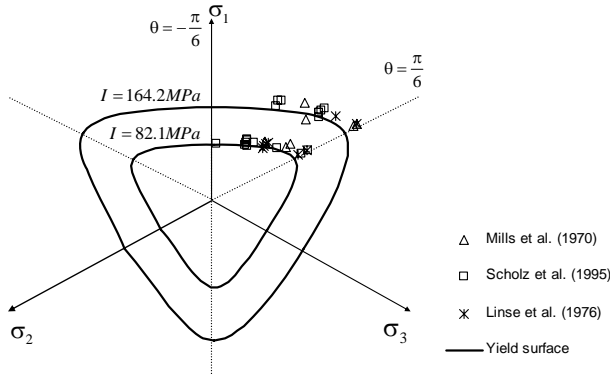


Figure 3. Comparison of the yield surface with the experimental data in the deviatoric plane.

Simulations of triaxial compression tests with different confining pressures are performed. The simulations are compared with the laboratory tests. Figure 4 shows an example of simulation of triaxial compression tests and its comparison with experimental data reported by Kotsovos and Newman (Kotsovos & Newman 1980). This comparison shows that the proposed model is able to predict the main features observed in the laboratory tests.

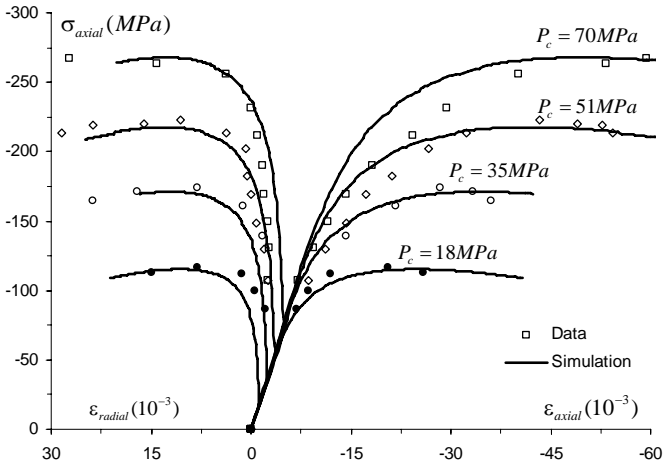


Figure 4. Triaxial compression tests with different confining pressures. Data reported by Kotsovos and Newman (Kotsovos & Newman 1980).

In addition to the previous simulations, some simulations are also realized for triaxial compression tests with low confining pressures. The experimental data is reported by Sfer et al. (Sfer et al. 2002). The comparison between the response of the model and the laboratory tests is presented in Figure 5. We notice that the proposed model is able to give good results for the basic features of concrete and for all stages of loading. It can describe the hardening phase correctly, the behaviour at ultimate stress state as well as the softening phase.

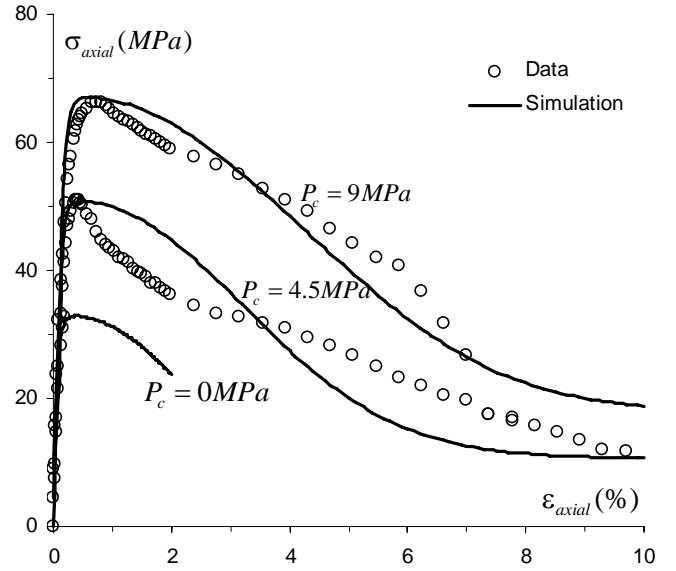


Figure 5. Triaxial compression tests with different confining pressures. Data reported by Sfer et al. (Sfer et al. 2002).

4 NON-LOCAL DAMAGE MODEL

In the local theory, the physical state of a point material depends only on the state of the material itself. The local formulation, using the finite element method, leads to mesh dependencies and severe difficulties in the softening regime. The strain and damage tends to localize into a band with finite width. The width of this band decreases for fine meshes and it tends to zero if the mesh is refined more and more. The governing equilibrium equations lose their ellipticity. This will lead to ill-posed boundary value problems. This mesh sensitivity is an open topic that leads many researchers to propose regularization approaches. One of the regularization approaches is the non-local approach. The non-local theory states that the local state of a point material is not sufficient to evaluate the stress at that point. This theory considers that the response of a point material depends on the deformation at that point as well as the deformation of the neighbourhood points. A material loses its resistance with damage. The increase of the damage can create a softening behaviour. In order to avoid the mesh dependency, the non-local approach is applied only for the variables that control the strain softening. So, the concept of non-locality is applied here only to the damage variable. The non-locality of damage is introduced through the definition of a weight average of the driving force ξ_d . The driving force is replaced with its average over a representative elementary volume V_r . The expression of the non-local driving force is the following:

$$\bar{\xi}_d(\vec{x}) = \frac{\int_{V_r} \xi_d(\vec{y}) dV}{V_r} \quad (21)$$

A Gauss type weight function $\psi(\vec{y}, \vec{x})$ is introduced in order to generalize the above integral over the whole domain Ω :

$$\bar{\xi}_d(\vec{x}) = \frac{1}{\Psi(\vec{x})} \int_{\Omega} \psi(\vec{y}, \vec{x}) \xi_d(\vec{y}) d\Omega \quad (22)$$

$\Psi(\vec{x})$ is a normalizing factor whose expression is given by:

$$\Psi(\vec{x}) = \int_{\Omega} \psi(\vec{y}, \vec{x}) d\Omega \quad (23)$$

The weight function is supposed to be homogeneous and isotropic. It depends on the distance between the source point \vec{x} and the receiver point \vec{y} . Many weight functions are presented in the literature. The Gaussian weight function is the most popular and used one:

$$\psi(\vec{y}, \vec{x}) = \left(\frac{1}{l\sqrt{2\pi}} \right)^{N_{\text{dim}}} \exp\left(-\frac{\|\vec{x} - \vec{y}\|^2}{2l^2} \right) \quad (24)$$

N_{dim} is the number of spatial dimensions. l is the characteristic length. The characteristic length depends on the heterogeneity of the material.

4.1 Implementation of the non-local variable

The non-local driving force of damage defined by the equation (22) can be calculated using Gauss method in the finite element method. The non-local value $\bar{\xi}_d$ over a geometric point vector \vec{x}_i is calculated as follows:

$$\bar{\xi}_d(\vec{x}_i) = \frac{\sum_{N=1}^{N_e} \sum_{g=1}^{N_g} w_g \psi(\vec{y}_g, \vec{x}_i) \xi_d(\vec{y}_g) \det(J)_g}{\sum_{N=1}^{N_e} \sum_{g=1}^{N_g} w_g \psi(\vec{y}_g, \vec{x}_i) \det(J)_g} \quad (25)$$

N_e is the total number of elements, N_g is the number of Gauss points within an element, \vec{y}_g is the vector of the integration points and w_g is the gauss integration weight coefficient.

We present in figure 6 an illustration of the averaging zone within a mesh, with the source and receiver points. The material point \vec{x}_i is affected by the points in a certain neighbourhood depending on the characteristic length. The far points have negligible influence on the point behaviour.

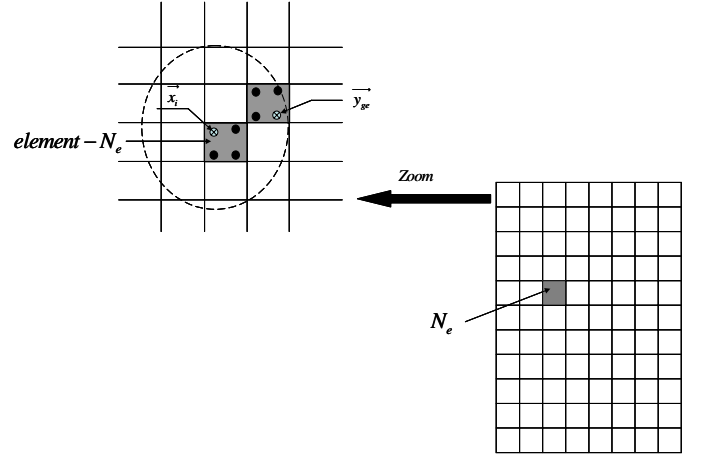


Figure 6. Illustration of averaging zone for non local damage model.

5 NUMERICAL APPLICATION

The model is implemented in a finite element code. In this section, we will show the performance of the proposed model in the modelling of the progressive failure after the strain localization. We will show the deficiency of the local formulation to reproduce correctly the strain localization phenomenon. Local and non-local analyses are thus performed for a structural example.

The example concerns the failure of a simply supported beam due to a vertical center point loading. The beam is of 3 m length and 0.3 m height. The vertical loading is controlled by applying a vertical displacement at the midpoint of the beam. This displacement varies from 0 to 1.5 cm. The geometry of the beam is illustrated in Fig. 7.

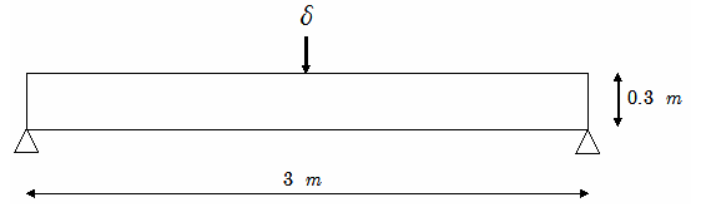


Figure 7. Geometry of the beam.

Three meshes of 300, 600 and 1200 elements are used to study the strain localization. We present the distribution of the damage in the beam using the local and non-local formulations. We notice that the results obtained by the local formulation are clearly sensitive to the mesh (Fig. 8). Due to the application of the vertical displacement, tensile stresses are generated in the lower part of the beam. This will lead to the formation of microcracks. The microcracks will thus form a band of localization where the damage is localized. The localized damage zone is formed at the centre of the beam. The growth and the propagation of damage are propagating from the lower part to the upper part of the beam. The bandwidth decreases when the mesh is refined. The damage tends to localize into more

and more narrow band with the refinement of the mesh.



Figure 8. Local damage distribution in the beam: (a)- 300 elements, (b)- 600 elements and (c)- 1200 elements.

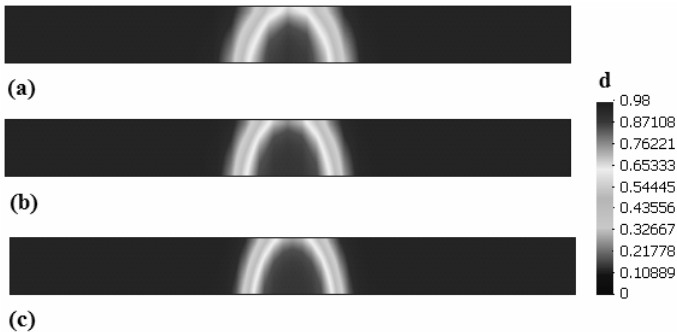


Figure 9. Non-local damage distribution in the beam: (a)- 300 elements, (b)- 600 elements and (c)- 1200 elements.

In Figure 9, we present the distribution of damage in the beam using the non-local model. We notice that the results are insensitive to the mesh used. The width of the damaged zone is controlled by the internal characteristic length. So, the non-local analysis is capable to regularize the problem of mesh sensitivity.

The damage profiles are plotted for the three meshes at the midheight of the beam along the horizontal axis. Once again, in the local study, the damage tends to localize into a narrow zone when the mesh is refined (Fig. 10).

On the other hand, the damage profiles obtained by the non-local analysis are almost identical for the three meshes (Fig. 11)

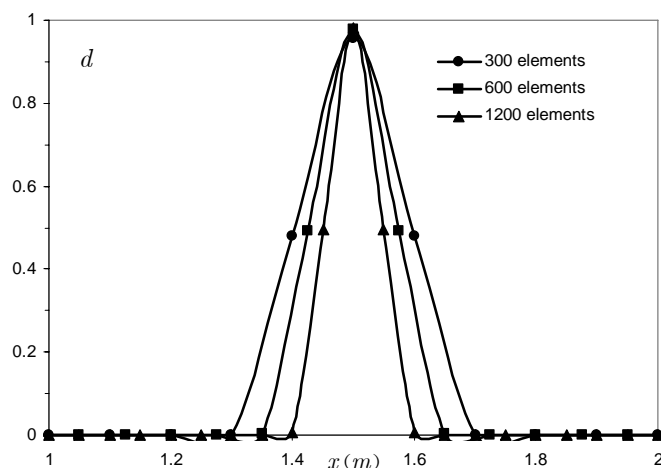


Figure 10. Local damage profiles at the midheight of the beam along x-axis.

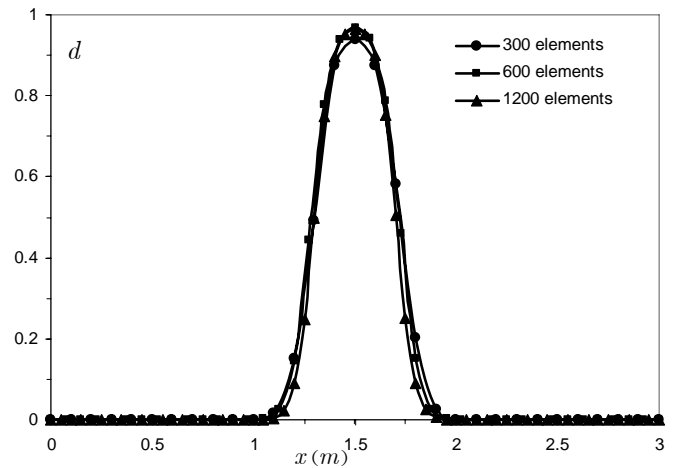


Figure 11. Non-local damage profiles at the midheight of the beam along x-axis.

We present, in figure 12, the vertical force-displacement curve at the centre of the beam for the three meshes using the nonlocal approach.

The results do not suffer from pathological sensitivity to mesh size. The curves are almost identical for fine meshes.

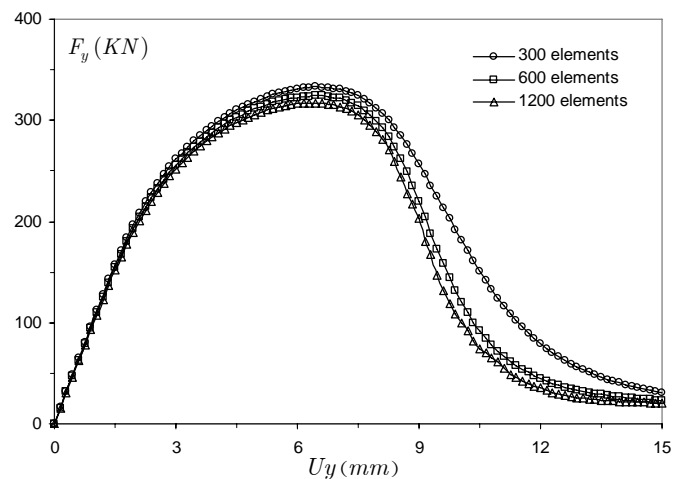


Figure 12. Vertical load-displacement curve at the centre of the beam using the nonlocal approach.

6 CONCLUSION

An elastoplastic model coupled with damage is formulated for the mechanical behaviour of concrete. The model is then applied for the simulation of some laboratory tests at different loading conditions. There is a good agreement between the numerical prediction of the model and the experimental data. The softening behaviour is controlled by the induced damage produced by microcracks. The model is then formulated in a non-local manner. The non-local approach is applied on the evolution of damage. The local driving force is replaced by its non-local counter part. Representative concrete structure was studied to

show the applicability of the model to engineering concerns. Local and non-local analyses are applied to a concrete beam subjected to a 3-point flexure. The local results are sensitive to the mesh. The width of the damaged zone decreases with the refinement of the mesh. Whereas, the results obtained by the non-local model are insensitive to mesh. The width of the damage zone is constant. This shows the performance of the non-local approach to well regularize the problem of strain localization.

REFERENCES

- Bazant, Z. P. & Pijaudier-Cabot, G. 1989. Measurement of Characteristic Length of Nonlocal Continuum. *Journal of Engineering Mechanics* 115(4), April, 1989.
- Borino, G., Failla, B. & Parrinello, F. 2003. A symmetric nonlocal damage theory. *International Journal of Solids and Structures* 40: 3621–3645.
- Hill, R. & Hutchinson, J.W. 1975. Bifurcation phenomena in the plane tension test, *J. Mech. Phys. Solids* 23: 239-264.
- Imran, I. 1994. Applications of non-associated plasticity in modeling the mechanical response of concrete. *PhD. Thesis, Department of Civil Engineering, University of Toronto, Canada*, 208pp.
- Jirasek, M. & Rolshoven, S. 2003. Comparison of integral-type nonlocal plasticity models for strain-softening materials. *International Journal of Engineering Science* 41: 1553–1602.
- Kotsovos, M.D. & Newman, J.B. 1980. Mathematical description of deformational behavior of concrete under generalized stress beyond ultimate strength. *Journal of the American Concrete Institute – ACI* 77 (5): 340–346.
- Linse, D. & Aschl, H. 1976. Versuche zum Verhalten von Beton unter mehrachsiger Beanspruchung. In *München durchgeführtes Teilprojekt eines internationalen Vergleichsprogrammes. Versuchsbericht, Lehrstuhl für Massivbau, Technische Universität München*.
- Mazars, J. 1984. Application de la mécanique de l'endommagement au comportement non linéaire et à la rupture du béton de structure. *Thèse de Doctorat d'Etat de l'Université Paris 6*.
- Mills, L. L. & Zimmerman, R. M. 1970. Compressive strength of plain concrete under multiaxial loading conditions. *ACI Journal* 67-47: 802–807.
- Mura T., 1987. Micromechanics of defects in solids. Second, revised edition, Martinus Nijhoff Publishers
- Pietruszczak, S., Jiang, J. & Mirza, F.A. 1988. An elastoplastic constitutive model for concrete. *Int J. Solids & Structures* 24 (7): 705-722.
- Pijaudier-Cabot, G. & Bažant, Z. P. 1987. Nonlocal Damage Theory. *Journal of Engineering Mechanics* (113)10: 1512-1533.
- Rodriguez-Ferran, A., Morata, I. & Huerta, A. 2004. Efficient and reliable nonlocal damage models. *Comput. Methods Appl. Mech. Engrg.* 193: 3431-3455.
- Scholz, U., Nechvatal, D., Aschl, H., Linse, D., Stockl, S., Grasser, E., Kupfer, H. 1995. Versuche zum Verhalten von Beton unter dreiachsiger Kurzeitbeanspruchung. *Deutscher Ausschuss für Stahlbeton, Heft 447, Berlin*, 64pages.
- Sfer, D., Carol, I., Gettu, R., & Etse, G. 2002. Study of the Behavior of Concrete under Triaxial Compression. *Journal of Engineering Mechanics* 128(2):156-163.

- Smith, S.H. 1985. On fundamental aspects of concrete behavior. *M. Sc. Thesis, Department of Civil Engineering, University of Colorado, USA*, 192pp.
- Willam, K.J. & Warnke, E.D. 1975. Constitutive model for the triaxial behaviour of concrete. *Proc. Int. Ass. For Bridge and Struct. Engrg.* 19, ISMES, Bergamo, 174-186.